Quantum Monte Carlo Device Simulation of Nano-Scaled SOI-MOSFETs

Tsuchiya, Hideaki

Horino, Motoki

Miyoshi, Tanroku

Quantum Monte Carlo Device Simulation of Nano-Scaled SOI-MOSFETs

Hideaki Tsuchiya, Motoki Horino and Tanroku Miyoshi
Department of Electrical and Electronics Engineering, Kobe University
1-1, Rokko-dai, Nada-ku, Kobe 657-8501, Japan

Abstract. **Quantum transport properties of nano-scaled SOI-MOSFETs are investigated based on a quantum Monte Carlo (MC) device simulation. The quantum mechanical effects are incorporated in terms of a quantum correction of potential in the well-developed particle MC computational techniques. The ellipsoidal multi-valleys of silicon conduction band are also considered in the simulation. First, the validity of the quantum MC technique is verified by comparing the simulated results with a self-consistent Schrödinger-Poisson solution at thermal equilibrium. Then, we apply the technique to non-equilibrium and quasi-ballistic quantum transport in nano-scaled SOI-MOSFETs.**

Key Words. **nano-scale MOSFET, quantum transport, ballistic transport, quantum Monte Carlo**

1. Introduction

As the channel length of MOSFETs approaches the thickness of inversion-layer, we have to control quantized effects to realize ultimate device performance. Although the quantized effects of two-dimensional (2D) electron gas in inversion-layer reduce the gate capacitance, they can enhance low-field mobility and increase inversion-layer capacitance if the subband structures are designed properly [1]. When the channel length is further shortened less than or comparable to a carrier's mean free path, the frequency of scattering events in these ultra-small devices is diminished, so that we will need to consider its ballistic behavior even at the room temperature operation [2]. The quantum hydrodynamic approaches [3,4] based on classical parameters, such as mobility and relaxation time, will not be applicable to investigate such a ballistic behavior.

In this paper, we will present a quantum transport modeling of nano-scaled SOI-MOSFETs by using a quantum Monte Carlo (MC) device simulation [5,6]. The quantum mechanical effects are incorporated in terms of a quantum correction of potential in this particle model. The ellipsoidal multi-valleys of silicon conduction band are also considered in the transport simulation, which is very important in the practical design of nano-scaled MOSFETs, but may not be taken into account in the alternative quantum MC approach based on the effective potential [7]. First, we will demonstrate the validity of the quantum MC technique at thermal equilibrium. Then, we will apply the technique to the non-equilibrium electron transport in nano-scaled SOI-MOSFETs, where a quasi-ballistic behavior of ultra-short channel devices is studied by evaluating the frequency of carrier scattering events in channel region.

2. *Quantum Monte Carlo Technique*

By taking the lowest-order quantum correction in the Wigner transport equation and supposing that the system is close to equilibrium [6,8], we have derived a quantum-corrected Boltzmann transport equation as follows.

$$\frac{\partial f}{\partial t}+\sum_{i=x,y,z}\frac{\hbar k_i}{m_i^*}\frac{\partial f}{\partial r_i}-\frac{1}{\hbar}\nabla_{\mathbf{r}}\left(U+U^{QC}\right)\cdot\nabla_{\mathbf{r}}f=\left(\frac{\partial f}{\partial t}\right)_C \qquad (1)$$

where the quantum mechanical effects are incorporated in terms of a quantum correction of potential, which is represented in case of a 2D Si-MOSFET by

$$U_v^{QC}=-\frac{\hbar^2}{12m_x^v}\frac{\partial^2\ln(n_v)}{\partial x^2}-\frac{\hbar^2}{12m_y^v}\frac{\partial^2\ln(n_v)}{\partial y^2} \qquad (2)$$

where the index v denotes the numbers of 1, 1', 2, 2', 3 and 3', which correspond to the six equivalent valleys

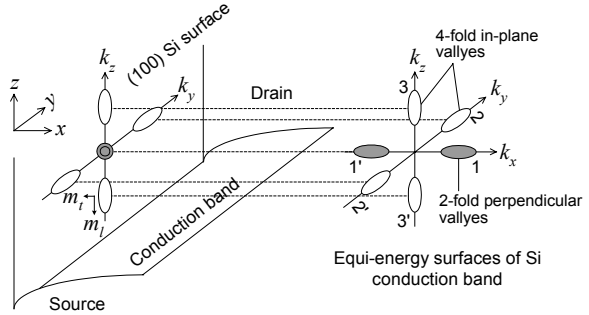

Fig. 1. Schematic diagram for equi-energy surfaces of conduction band in Si MOS interface.

of Si conduction band as shown in Fig. 1. n_v represents the carrier densities, and m_x^v and m_y^v the effective masses of the ellipsoidal energy bands. Here, we have to add that the effective masses are not treated as fitting parameters, and taken as those original values of $m_l = 0.98m_0$ and $m_t = 0.19m_0$ in the present simulation. From eq. (1), the following equations of motion are found to govern the particles in free flight.

$$\frac{d\mathbf{r}}{dt} = \mathbf{v} \ , \quad \frac{d\mathbf{k}}{dt} = -\frac{1}{\hbar}\nabla_r (U + U_v^{QC}) \qquad (3)$$

Further, in the calculation of the transition rates of scattering processes, the quantum correction of potential U_v^{QC} should be taken into account in the evaluation of the carrier's total energy. We have already demonstrated that the quantum MC technique proposed works well to describe the quantum transport problems including tunneling and quantum confinement effects [5,6,8], and also have carried out a detailed comparative study with the effective potential approach for a one-dimensional tunneling barrier [5].

3. *Thermal Equilibrium Solutions*

The 2D device model used in the simulation is shown in Fig. 2. The channel region is assumed to be intrinsic

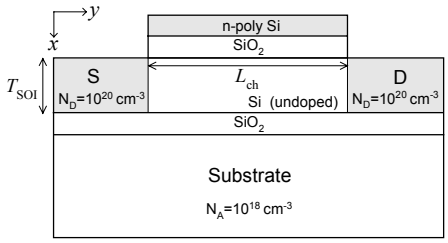

Fig. 2. Simulation model. The channel region is undoped and perfectly uniform.

and perfectly uniform. As for the scattering mechanism, only phonon scattering is taken into account in the channel region, where both intra-valley acoustic phonon and inter-valley phonon scattering including *f*-phonons and *g*-phonons are incorporated [9]. Impurity scattering is considered only in the source and drain regions. The gate oxide thickness is 1.5nm, where the gate tunneling effect is neglected in this study. The temperature is 300K.

Fig. 3 shows the calculated inversion electron distributions in the *x* direction, which are extracted in the middle of the channel, for (a) T_{SOI} = 3nm and (b) T_{SOI} = 2nm. The gate voltage V_G is 1.0V and the drain voltage V_{DS} is set 0V to obtain thermal equilibrium solutions. The channel length was set to be sufficiently long (=50nm), where the 2D quantum MC simulation is carried out. The results obtained by using a one-dimensional self-consistent SP solver are also plotted

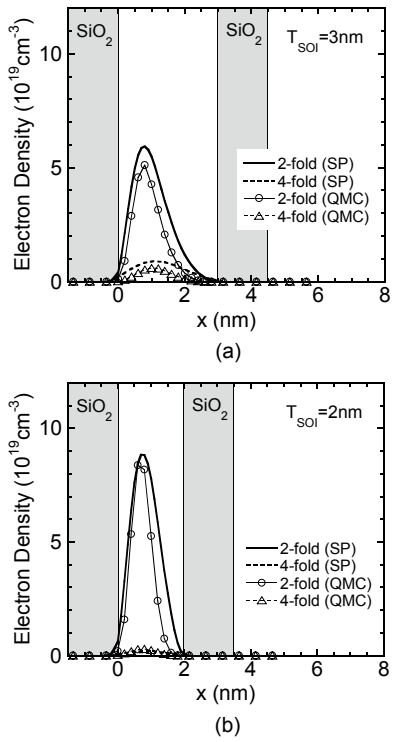

Fig. 3. Calculated inversion electron distributions in the x direction for (a) T_{SOI} = 3nm and (b) T_{SOI} = 2nm. The electron densities for 2-fold and 4-fold valleys are plotted separately. The gate voltage V_G is 1.0V and the drain voltage V_{DS} is set 0V. QMC and SP denote the quantum MC and the Schrödinger-Poisson methods, respectively.

for comparison. They agree quite well with the quantum MC solutions. The solid and the dashed lines represent the electron density distributions for the 2-fold and the 4-fold valleys, respectively. First, it is found that the higher electron occupancy of the 2-fold valleys is obtained even in the quantum MC method, which indicates that the subband energy difference between the 2-fold and the 4-fold valleys is effectively incorporated via the quantum correction of potential. Furthermore, we can confirm that the electron occupancy of the 2-fold valleys enhances when the SOI layer becomes thinner than the inversion-layer thickness [1]. The above results demonstrate that the quantum MC technique is sufficiently applicable to the quantum transport problems in ultra-thin SOI devices.

4. *Non-Equilibrium Quantum Transport*

Next, we study non-equilibrium electron transport when the drain bias voltage is applied. The SOI layer thickness is taken as 3nm, and the channel length L_{ch} 10nm. Fig. 4 shows (a) the integrated electron density and (b) the average electron velocity along the channel, where $V_G = V_{DS} = 0.5$V and the channel region extends from y = 5 to 15nm. The solid and the dashed lines

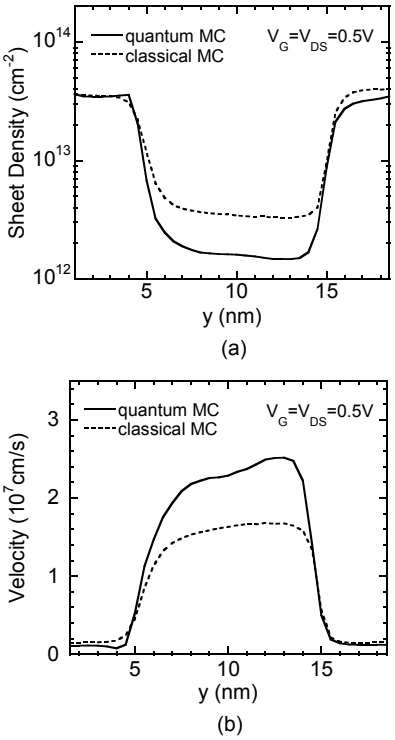

Fig. 4. (a) Integrated electron density and (b) average electron velocity along the channel at $V_G = V_{DS} = 0.5V$. The channel region is y = 5 to 15nm. The solid and the dashed lines correspond to the quantum MC and the classical MC methods, respectively, where the "classical" means that the quantum correction of potential is not included.

correspond to the quantum MC and the classical MC methods, respectively. The integrated electron density in the quantum MC method is reduced due to the quantum mechanical quantization in the inversion-layer. Here, it is worth noting that the average velocity of electrons evaluated by the quantum MC method is larger than that of the classical method. As mentioned before, the electrons in the channel region mainly stay at the 2-fold valleys with the lowest quantized subband. Since they have the lower conductivity effective mass and the higher mobility along the channel, the quantum

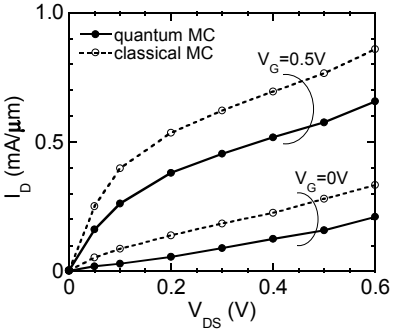

Fig. 5. Computed drain current-voltage characteristics for gate voltages of 0.5V and 0V. The solid and the dashed lines correspond to the quantum MC and the classical MC methods, respectively.

mechanically calculated mean velocity becomes larger compared to the classical simulation. Incidentally, such a carrier mean velocity increase due to the subband splitting has not been reported in the effective potential based quantum MC approach [7]. We have confirmed that due to the mean velocity increase, the average electron energy is also larger than the classical result. Fig. 5 shows the computed drain current-voltage characteristics for the gate voltages of 0.5V and 0V. Even though the average electron velocity increases in the quantum mechanical simulation due to the subband energy splitting, the drain current becomes lower than that of the classical simulation. The decrease in drain current is largely due to the reduction of electron density in the inversion-layer as shown in Fig. 4 (a).

To see the contribution of electrons in the 2-fold and the 4-fold valleys to the drain current in detail, the drain current-voltage characteristics for each valley are computed separately as shown in Fig. 6, where (a) and (b) correspond to the quantum MC and the classical MC methods, respectively. In the classical simulation of Fig. 6 (b), the current flowing through the 4-fold valleys is larger than that through the 2-fold valleys, which is simply due to the valley degeneracy of bulk silicon. On the other hand, the drain current in the quantum mechanical simulation is mainly governed by the 2-fold valleys as shown in Fig. 6 (a). This is due to the higher electron occupancy of the 2-fold valleys

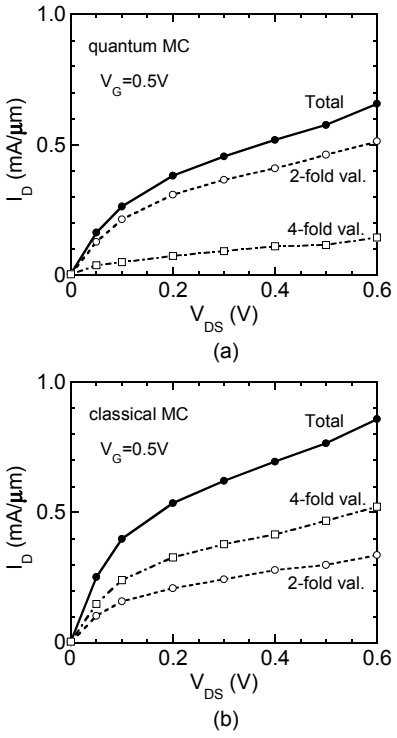

Fig. 6. Computed drain current-voltage characteristics for 2-fold and 4-fold valleys at $V_G = 0.5V$, where (a) and (b) correspond to the quantum MC and the classical MC methods, respectively. The total currents are also plotted by the solid lines.

caused by the subband energy splitting. Thus, a detailed modeling of 2D quantum effects considering the multi-valley structure in silicon conduction band is indispensable to analyze the non-equilibrium electron transport in nano-scaled Si-MOSFETs.

5. *Quasi-Ballistic Transport*

Next, we discuss quasi-ballistic behaviors of ultra-short channel devices. In the MC method, we can readily count frequency that a carrier encounters scattering in the course of traveling from source to drain. We have obtained the probability distributions of scattering numbers as shown in Fig. 7, where $V_G = V_{DS} = 0.5$V and only phonon scattering is taken into account. The channel length is varied from 5 to 30nm. The horizontal axis denotes the number of scattering events counted in the channel region and the vertical axis represents the corresponding probability. As a matter of course, the longer the channel is, the more the scattering happens. It is also found that only several

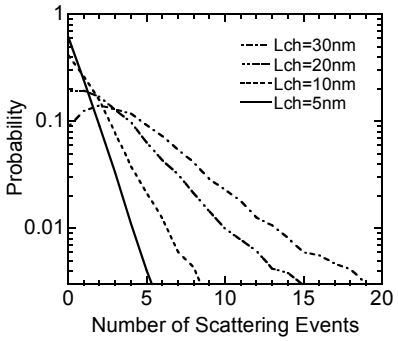

Fig. 7. Probability distributions of number of scattering events at $V_G = V_{DS} = 0.5V$.

scatterings are detected in the 5nm device, where about 60 percent of electrons are transferred from source to drain without any scattering. In other words, about 40 percent of electrons encounter at least one scattering event even in the 5nm channel.

Next, Fig. 8 shows the fraction of ballistic electrons and average number of scattering events computed as a function of channel length. The results by using the classical MC method are also plotted by the dashed lines. It is found from the quantum MC simulation that the ballistic electrons dominate more than half of the whole electrons when the channel length becomes less than 10nm. As a result, the average number of scattering events is estimated to be less than one for the sub-10nm channels. As shown in Fig. 4 (b), the classical particles are traveling the channel with slower mean velocity, and thus they encounter more scattering events until arriving at the drain electrode. Therefore, the ballistic behaviors of electrons are underestimated in the classical simulation as shown in Fig. 8.

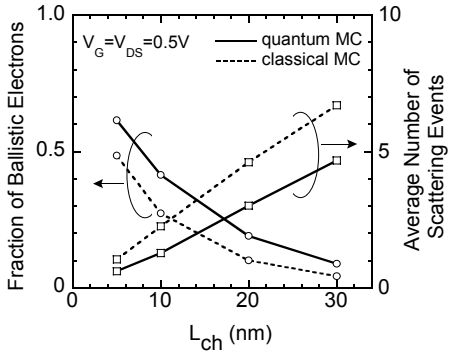

Fig. 8. Fraction of ballistic electrons and average number of scattering events as a function of channel length. $V_G = V_{DS} = 0.5V$. The results by using the classical MC method are also plotted by the dashed lines.

6. *Conclusion*

We have investigated the quantum transport properties of nano-scaled SOI-MOSFETs based on the quantum Monte Carlo technique. First, the validity of the technique is verified by simulating the thermal equilibrium electron distributions in the inversion-layer. Then, we have demonstrated that the multi-valley structure of silicon conduction band plays an important role in the non-equilibrium and quasi-ballistic transport of nano-scaled MOSFETs. We have also estimated the number of scattering events in ultra-short channel devices. We have found that a majority of electrons can be ballistic when the channel length shrinks less than 10nm. We hope that the quantum Monte Carlo technique will be a powerful tool for practical design of ultimate integrated devices.

Acknowledgments

This work is partially supported by the project of STARC and grant-in-aid by the Ministry of Education, Culture, Sports, Science and Technology (No. 13750061).

References

[1] S. Takagi, J. Koga, and A. Toriumi, Jpn. J. Appl. Phys. 37, 1289 (1998)
[2] K. Natori, IEICE Trans. Electron., E84-C, 1029 (2001).
[3] M. Ancona and G. Iafrate, Phys. Rev., B39, 9536 (1989).
[4] J. R. Zhou and D. K. Ferry: IEEE Trans. Electron Devices, 39, 473 (1992).
[5] M. Ogawa, H. Tsuchiya, and T. Miyoshi, IEICE Trans. Electron., E86-C, 363 (2003).
[6] H. Tsuchiya and U. Ravaioli, J. Appl. Phys., 89, 4023 (2001).
[7] D. Ferry, R. Akis, and D. Vasileska, Tech. Dig. Int. Electron Devices Meeting, San Francisco, 287 (2000).
[8] H. Tsuchiya and T. Miyoshi, IEICE Trans. Electron., E82-C, 880 (1999).
[9] C. Jacoboni and L. Reggiani, Rev. Mod. Phys., 55, 645 (1983).